Molecular Microbiology (2006) **61**(3), 704–722

doi:10.1111/j.1365-2958.2006.05235.x
First published online 27 June 2006

Pdr1 regulates multidrug resistance in *Candida glabrata*: gene disruption and genome-wide expression studies

John-Paul Vermitsky,[1] Kelly D. Earhart,[2] W. Lamar Smith,[1] Ramin Homayouni,[3] Thomas D. Edlind[1]* and P. David Rogers[2]

[1]*Department of Microbiology and Immunology, Drexel University College of Medicine, Philadelphia, PA, USA.*
[2]*Department of Pharmacy and Pharmaceutical Sciences, College of Pharmacy, and Department of Pediatrics, College of Medicine, University of Tennessee Health Science Center, Children's Foundation Research Center at Le Bonheur Children's Medical Center, Memphis, TN, USA.*
[3]*Department of Neurology, College of Medicine and Center for Genomics and Bioinformatics, University of Tennessee Health Science Center, Memphis, TN, USA.*

Summary

Candida glabrata **emerged in the last decade as a common cause of mucosal and invasive fungal infection, in large part due to its intrinsic or acquired resistance to azole antifungals such as fluconazole. In *C. glabrata* clinical isolates, the predominant mechanism behind azole resistance is upregulated expression of multidrug transporter genes *CDR1* and *PDH1*. We previously reported that azole-resistant mutants (MIC $\geq$ 64 μg ml^{-1}) of strain 66032 (MIC = 16 μg ml^{-1}) similarly show coordinate *CDR1-PDH1* upregulation, and in one of these (F15) a putative gain-of-function mutation was identified in the single homologue of *Saccharomyces cerevisiae* transcription factors Pdr1–Pdr3. Here we show that disruption of *C. glabrata PDR1* conferred equivalent fluconazole hypersensitivity (MIC = 2 μg ml^{-1}) to both F15 and 66032 and eliminated both constitutive and fluconazole-induced *CDR1-PDH1* expression. Reintroduction of wild-type or F15 *PDR1* fully reversed these effects; together these results demonstrate a role for this gene in both acquired and intrinsic azole resistance. *CDR1* disruption had a partial effect, reducing fluconazole trailing in both strains while restoring wild-type susceptibility (MIC = 16 μg ml^{-1}) to F15. In an azole-resistant clinical isolate, *PDR1* disruption reduced azole MICs eight- to 64-fold with no effect on sensitivity to other antifungals. To extend this analysis, *C. glabrata* microarrays were generated and used to analyse genome-wide expression in F15 relative to its parent. Homologues of 10 *S. cerevisiae* genes previously shown to be Pdr1–Pdr3 targets were upregulated (*YOR1*, *RTA1*, *RSB1*, *RPN4*, *YLR346c* and *YMR102c* along with *CDR1*, *PDH1* and *PDR1* itself) or downregulated (*PDR12*); roles for these genes include small molecule transport and transcriptional regulation. However, expression of 99 additional genes was specifically altered in *C. glabrata* F15; their roles include transport (e.g. *QDR2*, *YBT1*), lipid metabolism (*ATF2*, *ARE1*), cell stress (*HSP12*, *CTA1*), DNA repair (*YIM1*, *MEC3*) and cell wall function (*MKC7*, *MNT3*). These azole resistance-associated changes could affect *C. glabrata* tissue-specific virulence; in support of this, we detected differences in F15 oxidant, alcohol and weak acid sensitivities. *C. glabrata* provides a promising model for studying the genetic basis of multidrug resistance and its impact on virulence.**

Introduction

Increasing numbers of individuals are immunocompromised in association with AIDS, organ and tissue transplantation, aggressive treatments for cancer and immune-related diseases, diabetes, premature birth and advanced age. These individuals are at high risk for opportunistic fungal infection, in particular mucosal or systemic candidiasis. In the previous decade, *Candida glabrata* emerged as a common cause of these infections (10–30% of yeast isolates), trailing only *Candida albicans* (Pfaller *et al*., 1999; Safdar *et al*., 2001; Ostrosky-Zeichner *et al*., 2003; Richter *et al*., 2005). In some populations such as diabetics and the elderly, *C. glabrata* may be the dominant pathogen (Diekema *et al*., 2002; Kontoyiannis *et al*., 2002; Grimoud *et al*., 2005; Goswami *et al*., 2006). In *C. glabrata* candidaemia, mortality rates of 38–53% have been reported (Viscoli *et al*., 1999; Safdar and Armstrong, 2002; Klingspor *et al*., 2004). Nevertheless, the basis for *C. glabrata* pathogenicity is not yet clear, because it is deficient in the

Accepted 10 May, 2006. *For correspondence. E-mail tedlind@drexelmed.edu; Tel. (+1) 215 9918377; Fax (+1) 215 8482271.

virulence factors implicated in *C. albicans* infection: dimorphism, strong adhesion, secreted hydrolases and biofilm formation (Douglas, 2003; Nikawa *et al*., 2003; Kaur *et al*., 2005; Schaller *et al*., 2005). On the other hand, *C. glabrata* demonstrates relative resistance to azoles, the most widely used antifungal group which includes topical imidazoles such as miconazole and oral/parenteral triazoles such as fluconazole. Specifically, the fluconazole MIC inhibiting 50% of clinical isolates is 8 μg ml^{-1}, compared with 0.25 μg ml^{-1} for *C. albicans* (Ostrosky-Zeichner *et al*., 2003; Pfaller *et al*., 2004). Azoles inhibit lanosterol demethylase, product of the *ERG11* gene (*CYP51* in moulds), which results in depletion of the membrane component ergosterol and accumulation of toxic sterol products (for review, see Akins, 2005). The emergence of *C. glabrata* (from ≤ 5% of yeast isolates in the 1980s) parallels the introduction in the early 1990s of fluconazole and over-the-counter imidazoles, along with widespread application of agricultural azole fungicides. Indeed, its intrinsic low-level azole resistance, the molecular basis for which remains undefined, may represent a *C. glabrata* 'virulence factor'.

Candida glabrata also demonstrates a high capacity for acquired high-level azole resistance, with 8–27% of isolates demonstrating a fluconazole MIC ≥ 64 μg ml^{-1} (Safdar *et al*., 2002; Ostrosky-Zeichner *et al*., 2003; Pfaller *et al*., 2004). RNA analysis of these clinical isolates suggests that the predominant basis for acquired azole resistance is the constitutively upregulated expression of multidrug transporter genes *CDR1* and, to a lesser extent, *PDH1* (Miyazaki *et al*., 1998; Sanglard *et al*., 1999; 2001; Redding *et al*., 2003; Bennett *et al*., 2004; Vermitsky and Edlind, 2004; Sanguinetti *et al*., 2005). In support of this, *CDR1* or *CDR1-PDH1* disruption was shown to confer azole hypersensitivity (Sanglard *et al*., 2001; Izumikawa *et al*., 2003). In this respect, *C. glabrata* resembles *C. albicans* and other fungi in which azole resistance has been attributed to upregulated expression of multidrug transporters (Akins, 2005). Initial laboratory studies of *C. glabrata* acquired azole resistance using standard glucose-supplemented medium yielded avirulent respiratory-deficient mitochondrial mutants (Sanglard *et al*., 2001; Brun *et al*., 2005). Using glycerol-supplemented medium, we isolated respiratory-competent mutants with coordinately upregulated *CDR1-PDH1* analogous to that observed in azole-resistant clinical isolates (Vermitsky and Edlind, 2004). Coordinate upregulation of these genes was also observed following brief exposure of susceptible cells to azoles, representing a potential basis for intrinsic low-level resistance.

Coordinate *CDR1-PDH1* upregulation implies a common transcription factor. Although very distinct in terms of niche and human pathogenicity, *C. glabrata* is an evolutionary close relative of *Saccharomyces cerevisiae* (Barns *et al*., 1991; Dujon *et al*., 2004). In the latter, the coordinate upregulation of multidrug transporter genes *PDR5* and *SNQ2* is mediated by the paralogous Pdr1 and Pdr3 zinc cluster transcription factors (Kolaczkowska and Goffeau, 1999). Many gain-of-function mutations within Pdr1–Pdr3 have been identified that result in constitutive upregulation of *PDR5-SNQ2* along with a diverse group of additional genes (Carvajal *et al*., 1997; DeRisi *et al*., 2000; Devaux *et al*., 2001). Our analysis of the recently released *C. glabrata* genome sequence (Dujon *et al*., 2004) revealed a single *PDR1–PDR3* homologue, and a putative gain-of-function mutation in this gene was identified in azole-resistant laboratory mutant F15 (Vermitsky and Edlind, 2004). Here we demonstrate the central role of *C. glabrata PDR1* in acquired azole resistance, and identify a likely role in intrinsic resistance, by characterizing *Δpdr1* derivatives of laboratory strains and clinical isolates. Furthermore, we report the first application of microarrays to this organism, which identified multiple genes coregulated with *CDR1-PDH1* that are likely to impact *C. glabrata* virulence.

Results and discussion

PDR1 disruption in F15 and parent

The laboratory selection of spontaneous fluconazole-resistant mutants of *C. glabrata* ATCC strain 66032 was previously described (Vermitsky and Edlind, 2004). One of these mutants, F15, exhibited strong upregulation of *CDR1* and *PDH1*, modest upregulation of *PDR1*, and a single base change predicted to alter the Pdr1 amino acid sequence. We reasoned that disruption of *PDR1* in F15 and parent 66032 would provide an initial test of the hypothesis that this single base change is responsible for the fluconazole resistance. To accomplish this, *ura3* derivatives of F15 and 66032 were isolated by selection on 5-fluoroorotic acid (5FOA) and screening for complementation by a *URA3*-encoding plasmid. Homologous recombination is relatively non-specific in *C. glabrata*, especially with short homology regions, but can be enhanced by promoter-dependent disruption of genes (PRODIGE) as previously described (Edlind *et al*., 2005). This method was used to disrupt *PDR1* (Fig. 1A). Transformants were screened by polymerase chain reaction (PCR); loss of the PDR1uF-PDR1iR product and generation of the PDR1uF-URA3iR product confirmed *PDR1* disruption (Fig. 1B).

Broth microdilution assays were used to examine fluconazole susceptibility of F15*Δpdr1*, 66032*Δpdr1* and their parents (Fig. 1C). Similar to previous results with their parents (Vermitsky and Edlind, 2004), the 66032 and F15 *ura3* derivatives generated 24 h fluconazole MICs of 8–16 and > 64 μg ml^{-1} respectively. In contrast, their *Δpdr1* derivatives were fluconazole hypersusceptible, with

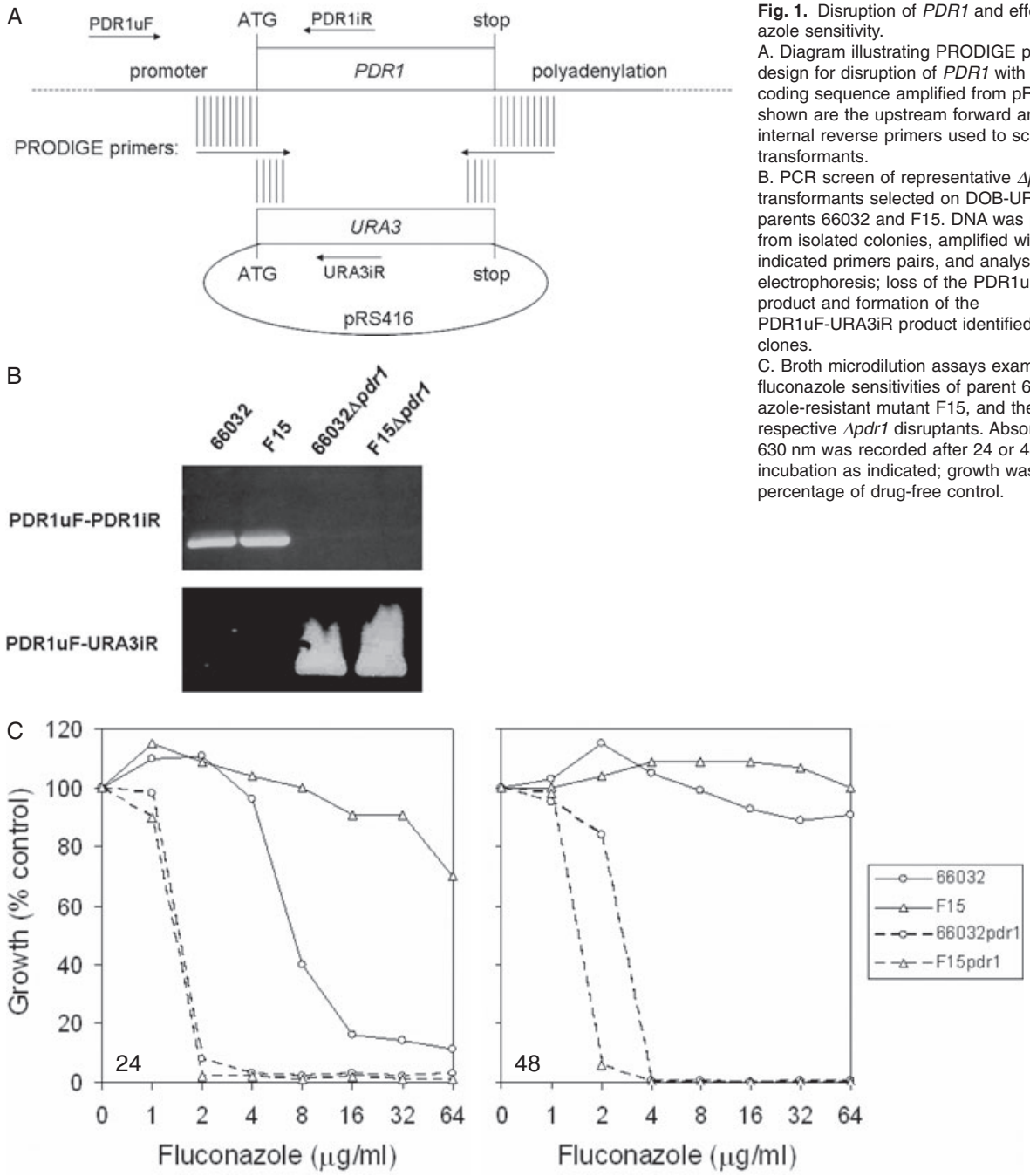

Fig. 1. Disruption of *PDR1* and effects on azole sensitivity.
A. Diagram illustrating PRODIGE primer design for disruption of *PDR1* with *URA3* coding sequence amplified from pRS416. Also shown are the upstream forward and two internal reverse primers used to screen transformants.
B. PCR screen of representative *Δpdr1* transformants selected on DOB-URA and their parents 66032 and F15. DNA was purified from isolated colonies, amplified with the indicated primers pairs, and analysed by gel electrophoresis; loss of the PDR1uF-PDR1iR product and formation of the PDR1uF-URA3iR product identified *Δpdr1* clones.
C. Broth microdilution assays examining fluconazole sensitivities of parent 66032, azole-resistant mutant F15, and their respective *Δpdr1* disruptants. Absorbance at 630 nm was recorded after 24 or 48 h incubation as indicated; growth was plotted as percentage of drug-free control.

equivalent MICs of 2 μg ml^{-1}. Although susceptible, 66032 exhibited trailing growth typical of many *Candida* species (Rex *et al*., 1998), and by 48 h was fully grown at all fluconazole concentrations tested (Fig. 1C). Trailing growth was absent in the *PDR1* disruptants. These results support the role of Pdr1 in F15 fluconazole resistance. Furthermore, the reduced MIC and trailing growth associated with *PDR1* disruption in 66032 suggests that Pdr1 is an important contributor to the intrinsic low-level resistance that is characteristic of this species.

As hypothesized, RNA analysis showed that *PDR1* disruption reversed the constitutive upregulation of *CDR1* and *PDH1* in untreated mutant F15 (Fig. 2). Moreover, expression of these genes was reduced relative to their expression in untreated parent 66032. This can explain the greater susceptibility of the *Δpdr1* derivatives relative to 66032. As previously described (Vermitsky and Edlind, 2004), fluconazole treatment induced the expression of *CDR1* and *PDH1*, most clearly in strains 66032 and F15 respectively (Fig. 2A). *PDR1* disruption completely

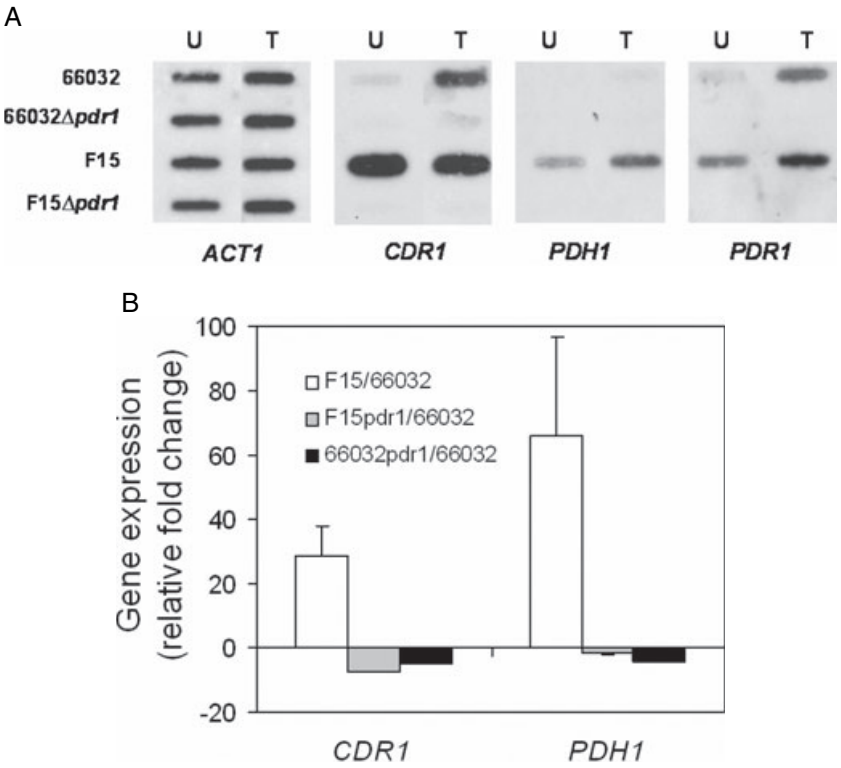

Fig. 2. Expression of multidrug transporter genes *CDR1* and *PDH1* and transcriptional activator gene *PDR1* in parent 66032, mutant F15 and their respective *Δpdr1* disruptants. A. RNA was isolated from log phase cultures, slot-blotted to membranes, and hybridized to the indicated gene probes; *ACT1* served as loading control. U, untreated cultures; T, treated with 256 μg ml^{-1} fluconazole for 2.5 h. B. Quantitative real-time RT-PCR analysis of relative *CDR1* and *PDH1* expression in F15 versus 66032, F15*Δpdr1* versus 66032, and 66032*Δpdr1* versus 66032. Data are shown as mean ± SD.

blocked this treatment-dependent upregulation. Finally, we note that *PDR1* itself, which is upregulated in F15 (Vermitsky and Edlind, 2004), is also induced by fluconazole treatment in 66032 and F15 (Fig. 2A).

CDR1 disruption

To more directly assess the role in acquired or intrinsic azole resistance of multidrug transporter gene *CDR1*, it was similarly disrupted in the *ura3* derivatives of 66032 and F15 (Fig. 3A). This reversed the fluconazole resistance of F15 (Fig. 3B), although the MIC (16 μg ml^{-1}) remained eightfold above that observed with *PDR1* disruption (Fig. 1C). With respect to 66032, *CDR1* disruption had minimal effect on fluconazole MIC at 24 h, but trailing growth most apparent at 48 h was eliminated as it was with *PDR1* disruption. These results are consistent with *CDR1* being a major but not exclusive contributor to F15 azole resistance.

PDR1 replacement

To rigorously test the role of F15 *PDR1* in azole resistance, we employed gene replacement. The 66032*Δpdr1* strain (see above) was transformed with PCR products representing wild-type and F15 *PDR1*, including 5′ and 3′ flanking sequences which should direct *PDR1* to its native locus (Fig. 4A). We initially attempted to select homologous recombinants on fluconazole-containing medium. However, this was precluded by a background of spontaneous fluconazole-resistant mutants in control (no added DNA) transformations (see below for further characterization of these mutants). As an alternative, the protein synthesis inhibitor cycloheximide is a known substrate for Cdr1-like multidrug transporters, and indeed *C. glabrata Δpdr1* strains are cycloheximide-hypersensitive (Edlind *et al.*, 2005). In contrast to fluconazole, cycloheximide-containing plates yielded no spontaneous mutants while five or six transformants were obtained with addition of wild-type or F15 *PDR1* respectively. PCR screening of these transformants confirmed homologous recombination into the native locus (Fig. 4B). All F15 *PDR1* replacements demonstrated fluconazole resistance comparable to F15 itself, while all but one of the wild-type *PDR1* replacements demonstrated wild-type sensitivity (Fig. 4C). Sequencing of a representative F15 *PDR1* replacement confirmed there were no mutations other than the previously described P927L (Vermitsky and Edlind, 2004).

Characterization of Pdr1-independent azole resistance

As noted above, a background of resistant mutants arose on fluconazole-containing YP-glycerol medium in control transformations of strain 66032*Δpdr1*, which involved plating *c.* 2×10^7 cells. To more rigorously examine this Pdr1-independent resistance, equivalent numbers

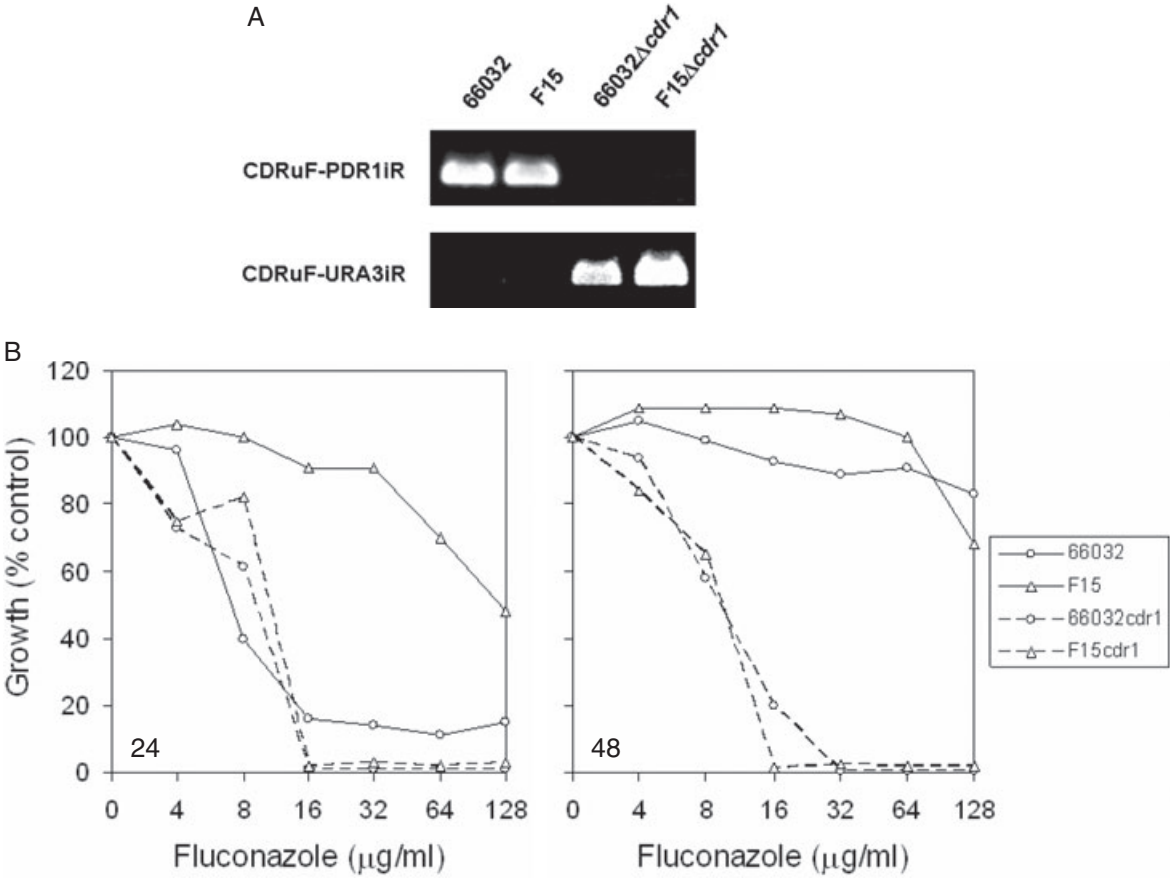

Fig. 3. Disruption of *CDR1* and effects on azole sensitivity.
A. PCR screen of representative *Δcdr1* transformants selected on DOB-URA and their parents 66032 and F15. DNA was purified from isolated colonies, amplified with the indicated primers pairs, and analysed by gel electrophoresis; loss of the CDR1uF-CDR1iR product and formation of the CDR1uF-URA3iR product identified *Δcdr1* clones.
B. Broth microdilution assays examining fluconazole sensitivities of parent 66032, azole-resistant mutant F15, and their respective *Δcdr1* disruptants. Absorbance at 630 nm was recorded after 24 or 48 h incubation as indicated; growth was plotted as percentage of drug-free control.

(3×10^5) of 66032 and 66032*Δpdr1* cells were plated on YP-glycerol medium with fluconazole ranging from 0 to 256 μg ml^{-1} (Vermitsky and Edlind, 2004). After 4 days incubation, the MIC was 32 μg ml^{-1} for 66032, and about 30 mutant colonies (frequency = 1×10^{-4}) were observed on each of the four plates at or above this concentration. With 66032*Δpdr1*, the MIC was 4 μg ml^{-1}, one or two colonies were observed at 4 and 8 μg ml^{-1}, and no colonies at 16–256 μg ml^{-1} (frequency $< 3 \times 10^{-6}$). Thus, Pdr1-independent azole resistance occurs at significantly reduced frequency.

PDR1 disruption in azole-resistant clinical isolates

Strain BG14, a model for *C. glabrata* pathogenesis (e.g. Domergue *et al*., 2005), is a *ura3* derivative of a clinical isolate from a patient who failed fluconazole therapy (Cormack and Falkow, 1999). Consistent with this, BG14 is fluconazole-resistant (MIC = 256 μg ml^{-1}), the molecular basis for which is unknown. *PDR1* disruption in BG14, conferring cycloheximide hypersensitivity, was previously reported (Edlind *et al*., 2005). Here we show that this disruption also largely reversed BG14 azole resistance. The fluconazole MIC decreased 16-fold to 16 μg ml^{-1} (Fig. 5A); i.e. comparable to the typical clinical isolate but eightfold above that observed for 66032*Δpdr1* (above). Ketoconazole, itraconazole and miconazole MICs were similarly reduced in BG14*Δpdr1*, but susceptibilities to unrelated antifungals terbinafine, caspofungin and amphotericin B were unchanged. Expression of *CDR1* and *ERG11* was examined by RNA hybridization (Fig. 5B). In BG14, constitutive expression of *CDR1* appeared to be modestly upregulated, but remained responsive to fluconazole-dependent upregulation. Both of these were strongly reduced in the *Δpdr1* derivative, while no effects on *ERG11* expression were observed.

Strain 8512 represents a second azole-resistant clinical isolate with high constitutive *CDR1-PDH1* expression (Ver-

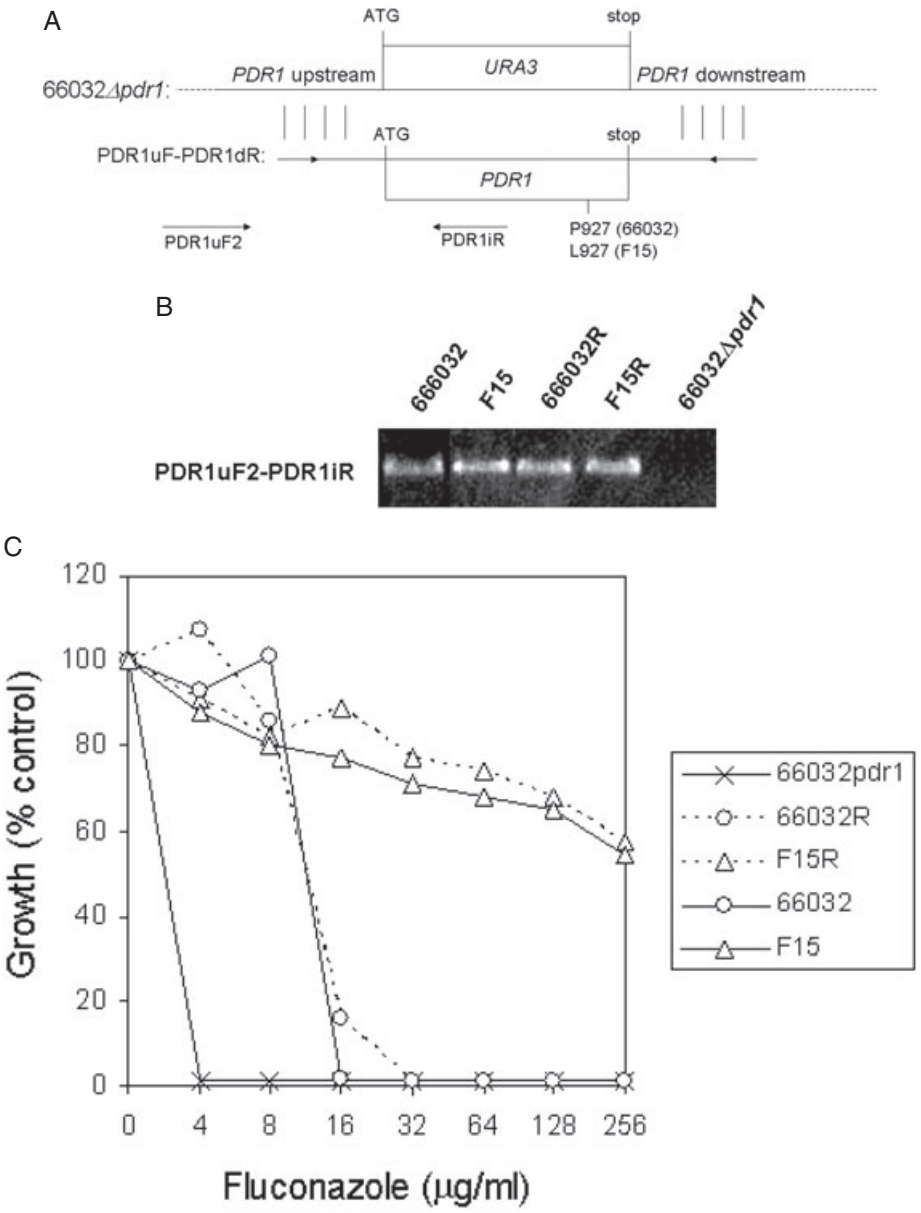

Fig. 4. *PDR1* replacement confirms role in azole resistance.
A. Diagram illustrating replacement and PCR screening strategies.
B. PCR screen of representative *PDR1* replacements 66032R and F15R (wild-type and F15-derived *PDR1*, respectively) selected on cycloheximide-containing plates, and their parent 66032*Δpdr1*; strains 66032 and F15 were included as positive controls. DNA was purified from isolated colonies, amplified with the PDR1uF2-PDR1iR primer pair, and analysed by gel electrophoresis; formation of product confirmed replacement of *PDR1* into its native locus in 66032*Δpdr1*.
C. Broth microdilution assay showing that replacement into 66032*Δpdr1* of 66032-derived (66032R) or F15-derived (F15R) *PDR1* conferred the expected low or high-level fluconazole resistance associated with 66032 and F15. Absorbance at 630 nm was recorded after 24 h incubation; growth was plotted as percentage of drug-free control.

mitsky and Edlind, 2004). Following 5FOA-mediated conversion to *ura3*, *PDR1* was disrupted in strain 8512 (not shown). Broth microdilution assays demonstrated reduction of fluconazole MIC from >256 to 32 μg ml^{-1}. Taken together, these data suggest that *PDR1* is a major determinant of azole sensitivity in *C. glabrata*, although additional gene mutations may contribute to clinical resistance.

Microarray analysis: upregulated genes

In light of the major role played by transcription activator gene *PDR1* in *C. glabrata* azole sensitivity, an examination of genome-wide changes in gene expression in mutant F15 was warranted. We first attempted this with *S. cerevisiae* microarrays, because these two yeast are

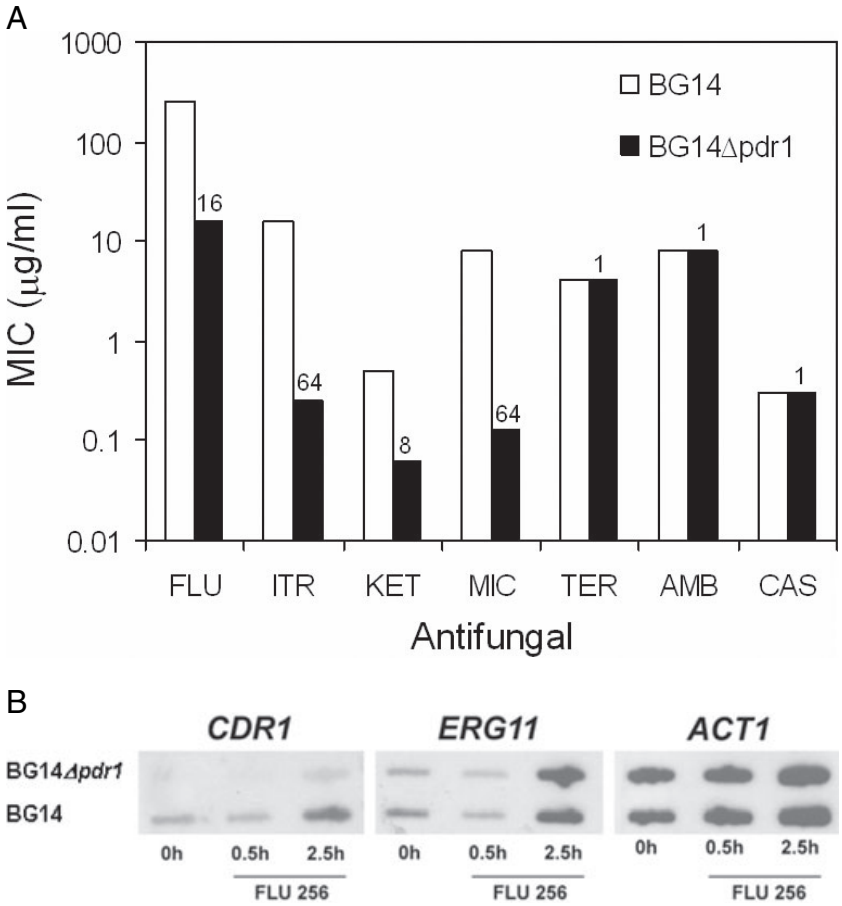

Fig. 5. Antifungal sensitivities and *CDR1-ERG11* expression in a *Δpdr1* derivative of azole-resistant clinical isolate BG14.
A. MIC values (at 24 h) determined by broth microdilution for BG14 and BG14*Δpdr1*. A log scale was used to facilitate comparison of MICs over a wide range. Numbers above the BG14*Δpdr1* bars indicate the fold-change relative to BG14. FLU, fluconazole; ITR, itraconazole; KET, ketoconazole; MIC, miconazole; TER, terbinafine; AMB, amphotericin B; and CAS, caspofungin.
B. RNA was isolated from log-phase BG14 and BG14*Δpdr1* cultures exposed to 256 μg ml^{-1} fluconazole for 0–2.5 h, slot-blotted to membranes, and hybridized to the indicated gene probes.

closely related. However, the only confirmable change was upregulation of the *PDR5* (18-fold) and *PDR15* (ninefold) homologues (data not shown); both of these genes share 73% nucleotide identity with *CDR1*.

Therefore, *C. glabrata* microarrays were developed for the Affymetrix platform (see *Experimental procedures*) and used to examine changes in F15 relative to 66032. In F15, 78 genes were upregulated ≥ twofold relative to 66032. These genes are listed in Table 1 , grouped by probable function and ordered by expression level. Among the upregulated are homologues of nine genes previously identified in microarray studies of *S. cerevisiae* Pdr1–Pdr3 gain-of-function mutants (DeRisi *et al*., 2000; Devaux *et al*., 2001). Five of these nine genes encode putative membrane proteins with roles in small molecule transport or lipid metabolism. These include, in addition to *CDR1* and *PDH1*, the upregulated genes *YOR1* involved in oligomycin efflux, *RSB1* involved in sphingoid base-resistance, and *RTA1* involved in 7-aminocholesterol resistance (see SGD website (http://www.yeastgenome.org) for further information on these genes and references).

The four remaining genes upregulated in both *S. cerevisiae* and *C. glabrata* gain-of-function mutants include *PDR1* itself (as previously reported; Vermitsky and Edlind, 2004), the stress-induced *RPN4* encoding a proteasome gene transcription factor, and the uncharacterized open reading frames (ORFs) *YLR346C* and *YMR102C*. The latter encodes a relatively large and evolutionarily conserved protein with a WD40 domain commonly found in signalling proteins, and its disruption has been associated with fluconazole resistance in *S. cerevisiae* (Anderson *et al*., 2003). The *YLR346C* product, in contrast, is not conserved; indeed, the *C. glabrata* and *S. cerevisiae* genes are not detectably homologous in terms of sequence but rather in terms of chromosomal synteny, flanked in both yeast by unambiguous *YLR345W* and *YLR347C* homologues. Also, both *YLR346C* products are short (101 and 112 amino acids) and highly charged in their C-terminal regions. In *S. cerevisiae*, *Ylr346c* is mitochondria-localized and forms a two-hybrid interaction with MAP kinase Slt2, suggesting a possible role in mitochondria-nucleus retrograde signalling.

Among the 69 genes whose upregulation appears to be *C. glabrata* F15-specific (i.e. not similarly upregulated in *S. cerevisiae*) are three additional homologues encoding small molecule transporters including quinidine and bile

Table 1. *C. glabrata gene*s upregulated ≥ twofold in fluconazole-resistant mutant F15.

Group	Systematic name	*S. cerevisiae* homologue[a]	*C. glabrata* designation	Description	Expression[b]		PDRE[c]
					F15	F15/66032	
Small molecule transport	IPF6352	[d]*PDR5*(*CDR1*)	CAGL0M01760g	ABC transporter involved in azole/multidrug resistance	41	2.5	134,298,388,516
	IPF9719	[d]*PDR15*(*PDH1*)	CAGL0F02717g	ABC transporter involved in azole/multidrug efflux	29	9.6	521,557
	IPF1620	*QDR2*	CAGL0G08624g	MFS transporter involved in quinidine/multidrug efflux	23	4.5	848
	IPF8922	[d]YOR1	CAGL0G00242g	ABC transporter involved in multidrug efflux	16	11	648
	IPF982	*YBT1*	CAGL0C03289g	ABC transporter involved in bile acid transport	13	7.7	450
	IPF3303	*OAC1*	CAGL0K11616g	Mitochondrial inner membrane transporter	4.7	2.5	839
Lipid, fatty acid, and sterol metabolism	IPF5152	[d]*RTA1*	CAGL0K00715g	Overexpression confers 7-aminocholesterol resistance	22	7.0	300,379
	IPF2180	*HFD1*	CAGL0K03509g	Putative mitochondrial fatty aldehyde dehydrogenase	13	5.6	218
	IPF4136	[d]*RSB1*	CAGL0L10142g	Sphingolipid flippase	12	2.8	641,881
	IPF8678	*LCB5*	CAGL0K05995g	Minor sphingoid long-chain base kinase	12	2.4	804
	IPF8367	*LAC1*	CAGL0M10219g	Ceramide synthase component	5.7	2.5	531
	IPF1002	*ARE1*	CAGL0C02981g	acyl-CoA:sterol acyltransferase; sterol esterification	4.6	4.6	114
	IPF4884	*ATF2*	CAGL0D05918g	Alcohol acetyltransferase; steroid detoxification	3.1	9.6	30,195,560,772
	IPF2739	*SPO14*	CAGL0L03135g	Phospholipase D	0.8	2.6	–
	IPF2620	*CSR1*	CAGL0D00946g	Phosphatidylinositol transfer protein	0.4	3.8	239
Cell stress	IPF6847	*HSP12*	CAGL0J04202g	Stress-induced membrane protein	29	4.0	849
	IPF3173	*YNL134c*	CAGL0K09702g	Alcohol dehydrogenase motif; stress-induced	14	9.5	541
	IPF4605	*YML131W*	CAGL0K12958g	Alcohol dehydrogenase motif, stress-induced	7.3	9.1	594
	IPF6629	*HSP31*	CAGL0C00275g	Possible chaperone and cysteine protease	3.5	2.0	–
	IPF4140	*YOR052C*	CAGL0L10186g	Uncharacterized; stress-induced	2.3	3.2	–
	IPF8736	*TPS3*	CAGL0H02387g	Trehalose-6-phosphate synthase/phosphatase subunit	1.5	4.4	–
	IPF5558	*HSP42*	CAGL0E00803g	Small cytosolic stress-induced chaperone	0.6	4.9	–
Transcription	IPF5076	[d]*RPN4*	CAGL0K01727g	Transcription factor for proteasomegenes	16	3.9	378,394,552
	IPF5932	*SUT1*	CAGL0I04246g	Transcription factor involved in sterol uptake	15	2.4	–
	IPF3325	[d]*PDR1*	CAGL0A00451g	Transcription factor involved in multidrug resistance	9.6	2.3	557,701
	IPF7202	*TAF9*	CAGL0M05005g	Subunit of TFIID and SAGA complexes	1.0	6.3	–
	IPF6366	*YPR013C*	CAGL0M01870g	Uncharacterized; potential zinc finger	0.8	2.9	–
	IPF2113	*SIP3*	CAGL0I01980g	Activates transcription through DNA-bound Snf1	0.4	2.2	–
	IPF118	*HOT1*	CAGL0H08866g	Transcription factor involved in osmostress response	0.1	4.9	228
DNA replication and damage response	IPF9036	YIM1	CAGL0M09713g	Implicated in DNA damage response	40	12	127,179
	IPF9035	*MEC3*	CAGL0M09735g	DNA damage checkpoint	1.6	15	110,162
	IPF2521	*DBF4*	CAGL0E04576g	Regulatory subunit of Cdc7p-Dbf4p kinase complex	0.7	2.4	–
	IPF785	*DPB3*	CAGL0B03355g	DNA polymerase II subunit	0.2	2.7	–
Protein synthesis, modification, or degradation	IPF3014	*OCH1*	CAGL0A01738g	Mannosyltransferase of *cis*-Golgi apparatus	5.2	2.5	–
	IPF6742	*UFD1*	CAGL0J08096g	Recognition of polyubiquitinated proteins	4.4	2.2	–
	IPF3846	*NCE3*	CAGL0G01540g	Carbonic anhydrase-like; non-classical protein export	3.1	2.9	–
	IPF3072	*RPN8*	CAGL0K08866g	Non-ATPase regulatory subunit of 26S proteasome	2.9	2.9	–
	IPF8484	*PCI8*	CAGL0M12749g	Possible shared subunit of Cop9 signalosome and eIF3	0.2	2.4	–
Vesicular and protein transport	IPF7414	*GSF2*	CAGL0L01485g	ER membrane, hexose transporter secretion	10	2.4	208
	IPF8257	*YPT52*	CAGL0G07689g	GTPase required for vacuolar protein sorting	1.6	2.8	–
	IPF8439	*MEH1*	CAGL0L02211g	Component of the EGO complex; microautophagy	0.5	5.7	–
	IPF4445	*VPS28*	CAGL0H05181g	Component of ESCRT-I complex; protein trafficking	0.5	2.2	–
	IPF4173	*VTI1*	CAGL0L10604g	Involved in *cis*-Golgi membrane traffic	0.3	6.7	741
	IPF3260	*GYL1*	CAGL0K10934g	putativegAP for Ypt1 involved in polarized exocystosis	0.3	4.0	–
	IPF271	*VPS51*	CAGL0H06809g	Golgi-associated retrograde protein complex	0.2	6.1	–

Table 1. *cont.*

Group	Systematic name	*S. cerevisiae* homologue[a]	*C. glabrata* designation	Description	Expression[b] F15	Expression[b] F15/66032	PDRE[c]
Signal	IPF1489	BAG7	CAGL0I07249g	GAP for Rho1; cell wall and cytoskeleton homeostasis	1.6	2.9	–
transduction	IPF8227	*CDC25*	CAGL0D06512g	Membrane bound GEF for Ras1-Ras2	1.2	5.8	–
	IPF351	*GAC1*	CAGL0F04917g	Regulatory subunit forglc7 protein phosphatase	0.9	4.7	–
	IPF2382	*YNL234W*	CAGL0J07502g	Similar toglobins with haem-binding domain	0.5	3.1	–
	IPF512	*GPG1*	CAGL0F07117g	Subunit of heterotrimericg protein, interacts withgrp1	0.4	2.6	–
	IPF5914	*KIN3*	CAGL0I04422g	Protein kinase	0.2	5.6	–
Mitochondrial	IPF2122	*FMP48*	CAGL0K04301g	Ser/Thr protein kinase; mitochondrial	11	2.8	–
	IPF7121	*YGR046W*	CAGL0G03861g	Essential protein involved in mitochondria transport	0.4	4.4	–
Cell wall	IPF9549	*FLO1*	CAGL0E00209g	Flo1-like family of cell wall proteins	2.6	3.0	284,419
Amino acid and	IPF496	*PYC1*	CAGL0F06941g	Pyruvate carboxylase isoform	4.6	2.3	–
carbohydrate	IPF4499	*STR3*	CAGL0L06094g	Cystathionine beta-lyase	0.7	5.0	–
metabolism	IPF5315	*MET8*	CAGL0K06677g	Bifunctional dehydrogenase and ferrochelatase	0.2	7.8	–
Chromatin/	IPF8319	*SMD3*	CAGL0M04631g	Core Sm spliceosome protein Sm D3	0.9	3.7	–
chromosome	IPF390	*SPC19*	CAGL0F05467g	Component of Dam1 spindle pole complex	0.5	13.1	–
structure	IPF8077	*SPC97*	CAGL0I02464g	Component of microtubule-nucleating Tub4 complex	0.5	2.8	–
	IPF2730	*SPC34*	CAGL0L03223g	Component of Dam1 spindle pole complex	0.4	2.5	–
Other metabolism	IPF6032		CAGL0M14091g	Putative quinone reductase/NADPH dehydrogenase	3.8	9.8	244,532
	IPF6034	*ADH6*	CAGL0M14047g	NADPH-dependent cinnamyl alcohol dehydrogenase	2.3	2.7	–
	IPF1279	*YPR1*	CAGL0A02816g	2-methylbutyraldehyde reductase	0.6	5.6	–
	IPF4182	*INP1*	CAGL0L10736g	Peripheral membrane protein of peroxisomes	0.2	5.5	–
Uncharacterized	IPF6116	YIL077C	CAGL0M12947g	Uncharacterized	20	38	472,502
	IPF8009	*YJL163C*	CAGL0M08426g	Uncharacterized; ARS in promoter	9.1	10	450
	IPF2520		CAGL0E04554g	Uncharacterized; no similarities	8.8	6.4	–
	IPF2196	[d]*YMR102C*	CAGL0K03377g	Transcribed along with MDRgenes by Yrr1/Yrm1	8.1	4.4	898
	IPF3019		CAGL0A01650g	Uncharacterized; no similarities	7.2	4.4	564
	IPF3875	[d]*YLR346C*	CAGL0G01122g	Uncharacterized; syntenic but minimal similarities	3.3	22	793,803
	IPF3655	*YLR177W*	CAGL0B01078g	Uncharacterized	2.7	2.5	–
	IPF1546		CAGL0G09603g	Uncharacterized; very weak similarity to Yor186w	2.1	6.1	–
	IPF2382	*YNL234W*	CAGL0J07502g	Similar toglobins with haem-binding domain	0.5	3.1	–
	IPF4149	*YOR059C*	CAGL0L10318g	Uncharacterized	0.5	2.4	–
	IPF6420	*YGR126W*	CAGL0I10604g	Uncharacterized	0.1	19	–
	IPF2249	*YHL010C*	CAGL0K02563g	Uncharacterized; mammalian BRAP2 homologue	0.1	5.0	–
	IPF9234		CAGL0M07766g	Uncharacterized; no similarities	0.1	4.0	–

a. Parentheses indicate a previously named *C. glabrata gene*.
b. Expression in *C. glabrata* 66032 is represented in arbitrary microarray units (for comparison, actin and β-tubulin gene homologues *ACT1* and *TUB2* had average expression levels of 66 and 8.6 respectively). F15/66032 represents the ratio of expression in the fluconazole-resistant mutant vs. its parent (for comparison, *ACT1* and *TUB2* had ratios of 0.6 and 0.8 respectively).
c. Promoter regions (900 bp) were searched for matches to the *S. cerevisiae* PDRE consensus TCCRYGSR. Numbers indicate the distance (in bp) upstream of the ATG start codon of the PDRE; hyphens (–) indicate the absence of a PDRE.
d. Genes similarly upregulated in *S. cerevisiae Pdr1–Pdr3* gain-of-function mutants (DeRisi *et al.*, 2000; Devaux *et al.*, 2001).

acid efflux protein genes *QDR2* and *YBT1*. Additional lipid metabolism genes include *ARE1* whose disruption in *S. cerevisiae* confers azole hypersensitivity (T. Edlind, unpubl. data) and *ATF2* involved in fatty acid and steroid detoxification. A third group of well-represented genes are involved in the cell stress response, including membrane protein gene *HSP12*, and *YML131W-YNL134C*; the latter two are unrelated by BLAST but share an ADH_zinc_N domain (identified by CD-search; Marchler-Bauer and Bryant, 2004) characteristic of zinc-dependent alcohol dehydrogenases-oxidoreductases. *YML131W-YNL134C* are also coordinately upregulated in *S. cerevisiae* in response to diverse stresses including heat, oxidizing agents, ethanol, nitrogen depletion and stationary phase (Gasch *et al*., 2000; see Expression Connection at http://www.yeastgenome.org). A similarly regulated *S. cerevisiae* gene is *GRE2*, also encoding an oxidoreductase and among the genes upregulated in Pdr1–Pdr3 gain-of-function mutants (DeRisi *et al*., 2000; Devaux *et al*., 2001). This provides an example of analogous but non-homologous genes upregulated in *C. glabrata* F15 and *S. cerevisiae* Pdr1–Pdr3 mutants.

Notable among the remaining upregulated genes with significant expression levels are: *SUT1* encoding a transcription factor involved in sterol uptake and hypoxic gene expression, *YIM1* implicated in DNA damage response, *OCH1* and *GSF2* involved in Golgi-ER functions, proteasome-related genes *UFD1* and *RPN8*, putative mitochondrial protein kinase gene *FMP48*, a quinone reductase-like gene curiously lacking in other fungal genomes but present in many bacteria and vertebrates, and the uncharacterized *YIL077C* whose product has been mitochondria-localized but interacts with a nuclear transcriptional complex.

Microarray analysis: downregulated genes

There were 31 genes downregulated ≥ twofold in F15 relative to parent 66032 (Table 2). Only one of these was also downregulated in *S. cerevisiae* Pdr1–Pdr3 gain-of-function mutants: membrane transporter gene *PDR12* involved in efflux of weak organic acids such as sorbate. Additional genes with significantly downregulated expression include zinc transporter gene *ZRT1*, major facilitator genes including *FLR1* implicated in fluconazole efflux, and homologues of cell surface protein genes *MUC1-EPA2* and *MKC7* implicated in adhesion and aspartic protease activity respectively. Finally, a gene was downregulated whose product has clear homology to the WRY family of putative membrane-anchored proteins previously identified only in *C. albicans* (unpublished annotation in NCBI database). This family has nine paralogues in *C. albicans* and seven in *C. glabrata* but none, surprisingly, in *S. cerevisiae*, suggesting a possible role in mammalian colonization.

Confirmation of microarray results

As our studies represent the first application of these *C. glabrata* microarrays, it was important to validate the results by independent methods. RNA blots or real-time reverse transcription (RT)-PCR were used to examine the expression of selected genes identified as upregulated in the microarray (other than already confirmed *CDR1*, *PDH1* and *PDR1*). For five of seven genes tested (*YLR346C*, *YOR1*, *YNL134C*, *YML131W* and *RTA1*), RNA blots confirmed F15 upregulation relative to the parent 66032 strain (Fig. 6A). The two exceptions (*MEC3* and *YJL163C*) represent genes whose expression in both parent and F15 were below the level of detection by RNA blot (not shown).

For all nine genes tested by real-time RT-PCR (*YOR1*, *RTA1*, *RPN4*, *QDR2*, *MET8*, *BAG7*, *CSR1*, *PDR1* and *YBT1*), the upregulation observed by microarray was confirmed (Fig. 5B). For most of these, the results were quantitatively similar; e.g. *YOR1* was upregulated 16-fold by microarray and 17-fold by RT-PCR and *CSR1* was upregulated 3.8-fold by microarray and 2.9-fold by RT-PCR. Expression of *ERG11* encoding the azole target lanosterol demethylase was essentially unaltered by RT-PCR (not shown), in agreement with microarray analysis (F15/66032 = 0.6) and RNA hybridization (Vermitsky and Edlind, 2004). One anomaly in the microarray analysis was the relatively low upregulation of *CDR1* (2.5-fold) compared with its high upregulation (*c*. 20-fold) in both RNA blots and RT-PCR (Fig. 2). Furthermore, Cdr1 was strongly upregulated on the protein level, as shown by SDS-PAGE of membrane preparations followed by mass spectrometric identification of eluted bands (Rogers *et al*., submitted for publication). Potential explanations for this anomaly include degradation or masking of the *CDR1* mRNA region targeted by the microarray, or a saturation effect due to the relatively high *CDR1* basal expression.

Promoter sequence analysis

To identify a candidate *C. glabrata* Pdr1 response element (PDRE), we took advantage of the F15 microarray data, the available genome sequence, and the evolutionary relatedness of this yeast to *S. cerevisiae*. The promoter regions (900 bp upstream of the start codon) for all genes listed in Tables 1 and 2 were searched for a match to the consensus *S. cerevisiae* PDRE (DeRisi *et al*., 2000; Devaux *et al*., 2001): TCC(GA)(CT)G(GC)(AG). At least one match to this sequence was identified in 31 of the 78 genes (40%) upregulated ≥ twofold. Moreover, one or more PDRE were identified in all nine genes upregulated in both *C. glabrata* and *S. cerevisiae* gain-of-function mutants, in

Table 2. *C. glabrata* genes downregulated ≥ twofold in fluconazole-resistant mutant F15 compared with parent 66032.

Group	Systematic name	*S. cerevisiae* homologue[a]	*C. glabrata* designation	Description	Expression[b]		PDRE[c]
					66032	F15/66032	
Small molecule transport	IPF5505	*ZRT1*	CAGL0E01353g	High-affinity zinc transporter	10	0.5	–
	IPF4392	*FLR1*	CAGL0H06017g	Multidrug efflux pump of major facilitator superfamily	6.1	0.4	–
	IPF6218	[d]*PDR12*	CAGL0M07293g	ABC transporter of weak organic acids	4.5	0.2	–
	IPF7808	*YHR048W*	CAGL0J00363g	Uncharacterized; major facilitator superfamily	2.2	0.4	–
	IPF867	*ATR1*	CAGL0B02343g	Multidrug efflux pump of major facilitator superfamily	1.8	0.4	–
	IPF1568	*SNG1*	CAGL0G09273g	Nitrosoguanidine resistance; putative transporter	1.3	0.1	–
Cell stress	IPF3249	*CTA1*	CAGL0K10868g	Catalase A	8.8	0.4	–
	IPF11021	*CRS5*	CAGL0H04257g	Copper-binding metallothionein-like protein	3.4	0.4	–
	IPF9018	*LTV1*	CAGL0J00891g	Required for growth at low temperature	1.0	0.4	656
	IPF9641	*SLG1*	CAGL0F01507g	Sensor of stress-activated Pkc1-Slt2 pathway	0.8	0.5	–
	IPF5937	*CUP2*(*AMT1*)	CAGL0I04180g	Metal-activated transcriptional factor	0.9	0.2	–
Carbohydrate metabolism	IPF986	*SDH2*	CAGL0C03223g	Succinate dehydrogenase iron-sulphur protein subunit	4.9	0.4	–
	IPF6117	*DOG2*	CAGL0M12925g	2-deoxyglucose-6-phosphate phosphatase	1.6	0.3	–
	IPF290	*PCK1*	CAGL0H06633g	Phosphoenolpyruvate carboxykinase	1.2	0.3	–
Cell cycle control	IPF2555	*SDS22*	CAGL0D00264g	Nuclear regulatory subunit ofglc7 phosphatase	0.3	0.2	–
RNA processing	IPF8796	*PNO1*	CAGL0K09460g	Nucleolar protein required for pre-rRNA processing	3.0	0.4	–
	IPF1130	*AAR2*	CAGL0A04543g	Component of the U5 snRNP	1.0	0.4	–
	IPF9324	*DIM1*	CAGL0L07678g	Essential 18S rRNA dimethylase	1.0	0.5	–
	IPF5272	*NOP8*	CAGL0B01397g	Nucleolar protein required for ribosome biogenesis	0.7	0.4	–
Cell surface and cytoskeleton	IPF9500	*MKC7*	CAGL0J01793g	Muc1/Epa2-like putative cell surface protein	4.2	0.3	–
	IPF8398		CAGL0E01771g	GPI-anchored aspartyl protease	3.6	0.3	–
	IPF807	*MNT3*	CAGL0B03003g	α-1,3-mannosyltransferase involved in O-glycosyltation	3.1	0.4	–
	IPF3539	*ECM4*	CAGL0G02101g	Promoter insertion mutant is calcofluor-hypersensitive	1.6	0.3	–
	IPF810	*MNT3*	CAGL0B02992g	α-1,3-mannosyltransferase involved in O-glycosyltation	1.4	0.3	–
	IPF821		CAGL0B02882g	*C. albicans* WRY family; transmembrane domain	0.5	0.1	–
	IPF5228	*ECM18*	CAGL0B01969g	Insertion mutant is calcofluor hypersensitive	0.3	0.3	–
	IPF7581	*TPM2*	CAGL0L08338g	Minor isoform of tropomyosin	0.3	0.4	–
Uncharacterized	IPF493	*YIR035C*	CAGL0F06897g	Uncharacterized; alcohol dehydrogenase domain	3.3	0.4	–
	IPF3428	*YNL095C*	CAGL0G06468g	Uncharacterized; related to *ECM3*	2.7	0.4	–
	IPF7665	*SIP5*	CAGL0L06864g	Uncharacterized; interacts withglc7 and Snf1	0.4	0.3	–
	IPF5688	*FMP16*	CAGL0G05269g	Uncharacterized; mitochondrial	0.3	0.3	–

a. Parentheses indicate a previously named *C. glabrata gene*.
b. Expression in *C. glabrata* 66032 is represented in arbitrary microarray units (for comparison, actin and β-tubulin gene homologues *ACT1* and *TUB2* had average expression levels of 66 and 8.6 respectively). F15/66032 represents the ratio of expression in the fluconazole-resistant mutant vs. its parent (for comparison, *ACT1* and *TUB2* had ratios of 0.6 and 0.8 respectively).
c. Promoter regions (900 bp) were searched for matches to the *S. cerevisiae* PDRE consensus TCCRYGSR. Numbers indicate the distance (in bp) upstream of the ATG start codon of the PDRE; hyphens (–) indicate the absence of a PDRE.
d. Genes similarly downregulated in *S. cerevisiae Pdr1–Pdr3* gain-of-function mutants (DeRisi *et al.*, 2000; Devaux *et al.*, 2001).

14 of 15 genes in the small molecule transport and lipid metabolism groups, and in 26 of 34 genes with expression level > 3 (arbitrary microarray units). Conversely, only one PDRE was identified among the 31 downregulated gene promoters (Table 2); similarly, none was identified in the promoters of representative housekeeping genes (*ACT1*, *TEF1*, *TDH3*) or azole target gene *ERG11*. This analysis therefore identifies TCC(AG)(TC)G(GC)(AG) as a strong candidate for the *C. glabrata* PDRE. More specifically, we note a clear preference for G as the penultimate base (95% of PDREs) and A as the final base (84%), although two of the four PDREs within the *CDR1* promoter have G as the final base.

Two exceptions warrant discussion. The promoters of *C. glabrata* upregulated genes *RPN8* and *YOR052C* lack a PDRE but include perfect matches to the *S. cerevisiae* Rpn4 transcription factor-binding site GGTGGCAAA (Mannhaupt *et al*., 1999); perfect or near-perfect matches are also found in the promoters of their *S. cerevisiae* homologues. As noted above, Rpn4 is upregulated in both *C. glabrata* Pdr1 and *S. cerevisiae* Pdr1–Pdr3 gain-of-function mutants. Thus, *RPN8-YOR052C* upregulation is likely Rpn4-mediated and only indirectly Pdr1-mediated.

Candida glabrata *F15 exhibits additional phenotypes predicted by microarray analysis which may alter virulence*

As coordinate *CDR1-PDH1* upregulation is commonly observed in *C. glabrata* azole-resistant clinical isolates (Bennett *et al*., 2004; Vermitsky and Edlind, 2004; Sanguinetti *et al*., 2005), the responsible mutations must have minimal effects on fitness. On the other hand, these mutations could alter *C. glabrata* in subtle ways that affect, for example, its relative virulence in the bloodstream versus mucosa. The F15 microarray results provided us with an opportunity to begin to test this general hypothesis. Specifically, we looked for phenotypes other than azole susceptibility predicted to be associated with altered expression of genes coregulated with *CDR1-PDH1*.

Upregulation of the *YOR1* transporter 11-fold (Table 1) predicts that azole-resistant F15 should be cross-resistant to oligomycin, an inhibitor of mitochondrial F_1F_0 ATPase and known *S. cerevisiae* Yor1 substrate. This was confirmed by broth microdilution assay (MIC = 0.5 μg ml^{-1} for F15 vs. 0.125 μg ml^{-1} for parent 66032), using medium with glycerol as respiratory carbon source. Yor1 also confers tolerance in *S. cerevisiae* to a wide range of organic anions such as leptomycin B and acetic acid, along with cadmium (Cui *et al*., 1996). *PDR12*, downregulated fivefold in F15, similarly encodes an efflux pump with specificity for organic acids, in particular sorbic acid (Piper *et al*., 1998). Spot assays (Fig. 7) confirmed sorbate hypersensitivity of F15, although the effects on MIC were modest (4 mM for F15 vs. 8 mM for 66032). With respect to organic acid sensitivity, *PDR12* downregulation may be largely offset by *YOR1* upregulation. There was no detectable change in sensitivity to acetic, boric, or lactic acids (MICs = 64, 16 and 250 mM respectively).

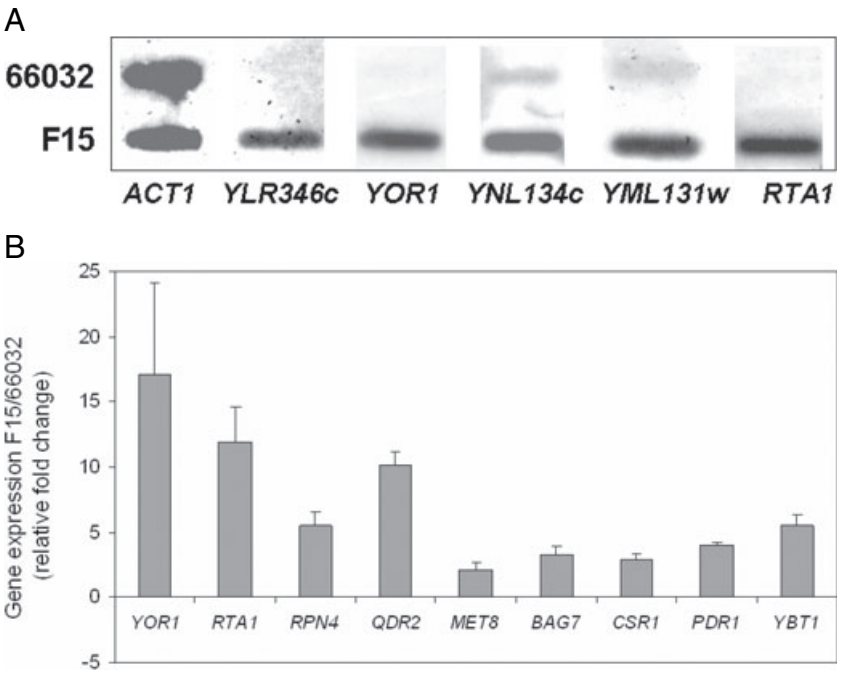

Fig. 6. Confirmation of F15/66032 microarray results for selected genes by RNA hybridization and real-time RT-PCR.
A. RNA was isolated from log phase cultures, slot-blotted to membranes, and hybridized to the indicated gene probes; *ACT1* served as loading control.
B. Quantitative real-time RT-PCR analysis of relative gene expression in F15 versus 66032. Data are shown as mean ± SD.

YML131W and *YNL134C* homologues were similarly upregulated *c.* ninefold in F15. As noted above, the products of these uncharacterized genes share a domain characteristic of alcohol dehydrogenases/oxidoreductases; furthermore, they are coregulated in response to environmental stresses including heat shock and treatment with reactive oxygen species or ethanol (Expression Connection, SGD website). Conversely, catalase gene *CTA1* was downregulated 2.5-fold. Consistent with this, F15 demonstrated hypersensitivity to hydrogen peroxide by spot assay (Fig. 7) and broth microdilution (MIC = 16 mM vs. 32 mM for 66032). Similarly, F15 demonstrated hypersensitivity to ethanol (Fig. 7; MIC = 2% vs. 4% for 66032). Equivalent results were obtained with F15 *PDR1* replacement clone F15R as compared with wild-type *PDR1* replacement clone 66032R (Fig. 7), confirming that these altered phenotypes resulted from the *PDR1* gain-of-function mutation. (Note that the *ura3* phenotype of 66032R can account for its variable growth relative to 66032, an effect also observed with the 66032 *ura3* strain; not shown.) Finally, we examined sensitivity to heat shock by exposing mid-log or early stationary phase cultures to 50°C for 10 min, following by plating on YPD with incubation at 35°C for 3 days to obtain colony counts. For F15 versus 66032, viability was 6 versus 0.3% and 16 versus 5% in log and stationary phase cultures respectively. Taken together, these data suggest that regulatory mutations conferring azole resistance in *C. glabrata* may have both positive and negative effects on fitness and virulence.

Conclusions

An important 'virulence factor' for the emerging opportunist *C. glabrata* appears to be its capacity for intrinsic low-level and acquired high-level azole resistance. The studies completed here with laboratory mutant F15, and initial studies with representative clinical isolates, identify the zinc cluster transcriptional activator Pdr1 as a key regulator of azole/multidrug transporter genes *CDR1* and *PDH1*. Constitutive upregulation of these genes is observed in most azole-resistant clinical isolates; furthermore, they are transiently upregulated in sensitive isolates following azole exposure. Consistent with this, in *PDR1* disruptants acquired resistance was reversed and intrinsic resistance was reduced. We have shown that F15 Pdr1 has a gain-of-function mutation analogous to those previously characterized in *S. cerevisiae* Pdr1–Pdr3, and this mutation is sufficient to confer azole resistance. Pdr1 mutation is not, however, necessary for resistance, because at least one resistant strain analysed had unchanged *PDR1* (Vermitsky and Edlind, 2004). Azole resistance may potentially arise from mutations in upstream signalling proteins or transcription cofactors, both of which remain to be defined (although histone modifying enzymes represent likely cofactors). Moreover, we observed here that *PDR1* disruptants, although azole hypersensitive, continued to yield spontaneous azole-resistant mutants at reduced frequency. These Pdr1-independent resistance mechanisms, and their clinical relevance, warrant further study.

Microarray analysis of genome-wide gene expression has become a central tool in molecular genetics, and the arrays developed and tested here should be particularly useful in studies of *C. glabrata* in large part because of its close evolutionary relatedness to *S. cerevisiae*. Most genes with altered expression in F15 had well-characterized *S. cerevisiae* homologues. This allowed us to predict F15 phenotypes, a number of which were tested including sensitivity to organic acids, alcohols and oxidants. Ultimately, these data should help us to

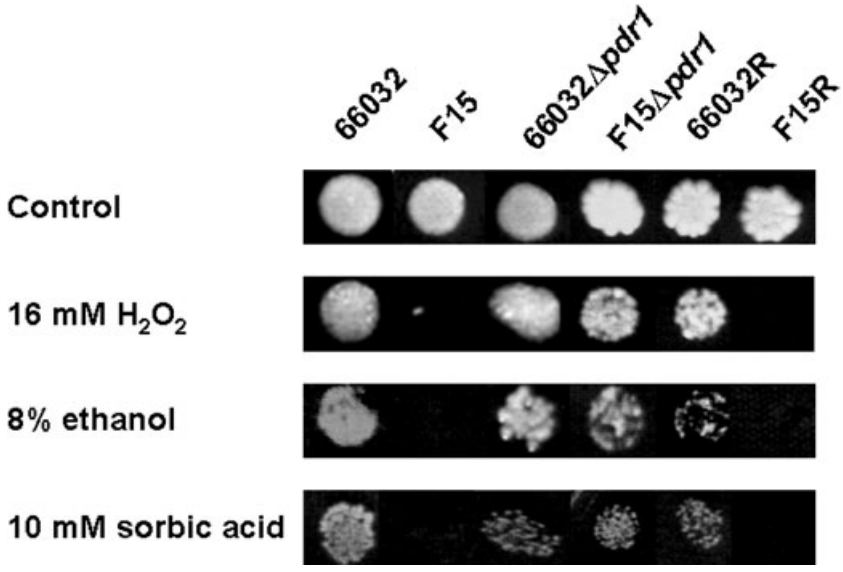

Fig. 7. Spot assays examining sensitivity of 66032 and its azole-resistant mutant F15 to hydrogen peroxide, ethanol and sorbic acid. Approximately 300 cells were spotted on YPD agar with the indicated inhibitor. Plates were incubated for 2–4 days at 35°C. For comparison, 66032Δ*pdr1*, F15Δ*pdr1* and the 66032Δ*pdr1-PDR1* replacement strains 66032R and F15R were examined in parallel.

understand and possibly exploit the consequences for *C. glabrata* of regulatory mutations leading to azole resistance. F15 hypersensitivity to hydrogen peroxide is of particular interest, because this implies hypersensitivity to immune cells such as neutrophils and environments such as the lactobacillus-colonized vaginal tract in which hydrogen peroxide plays an important role. Although the relatedness of *C. glabrata* and *S. cerevisiae* is invaluable in terms of predicting gene function, microarray analysis indicated that the Pdr1 and Pdr1-Pdr3 gain-of-function mutants of these yeast are more different than similar. This no doubt reflects the very different pressures placed on these organisms by their very different niches; e.g. the skin of a grape versus the human mucosa.

Following submission of this manuscript, Tsai *et al.* (2006) reported results that parallel and complement those described here. Specifically, a *C. glabrata* laboratory strain with transposon-disrupted *PDR1* exhibited fluconazole hypersensitivity and diminished *CDR1-PDH1* expression. Importantly, two fluconazole-resistant clinical isolates with increased *CDR1-PDH1* expression were shown to harbour *PDR1* mutations, and integrative transformation of these alleles conferred fluconazole resistance and upregulated *CDR1-PDH1* expression on the *pdr1::Tn* strain. These results confirm the relevance of laboratory mutant F15 as a model for clinical resistance.

Experimental procedures

Media, inhibitors and strains

For most experiments, the medium employed was YPD (1% yeast extract, 2% peptone, 2% dextrose). Gene disruptants and *ura3* mutants were selected on DOB (synthetic defined medium with dextrose) with complete supplement mixture (CSM) or CSM lacking uracil/uridine (-URA) (Qbiogene/BIO 101). Drugs were obtained from the following sources: fluconazole (Pfizer), itraconazole (Janssen), terbinafine (Novartis); caspofungin (Merck), amphotericin B, miconazole and cycloheximide (Sigma-Aldrich). They were dissolved in dimethyl sulphoxide (DMSO); the final DMSO concentration was $\leq$ 0.5% in all experiments which had no detectable effect on growth. Sorbic acid, lactic acid, acetic acid and hydrogen peroxide (Sigma) were diluted as necessary in water. Strains were previously described (Vermitsky and Edlind, 2004) or constructed as described below.

Isolation of ura3 strains

Wild-type *URA3* yeast strains are sensitive to 5FOA. To isolate 5FOA-resistant mutants, a single colony from a fresh YPD plate was streaked on DOB + CSM agar containing 0.1% 5FOA (Research Products International) and incubated at 35°C for 3 days. Colonies were streaked for isolation on YPD and DOB-URA; those that failed to grow on the latter were then tested for *URA3* complementation by transformation with pRS416 (shuttle vector with *S. cerevisiae URA3*) and selection on DOB-URA plates. Yeast transformations employed the Frozen-EZ Yeast Transformation II Kit (Zymo Research) as previously described (Edlind *et al.*, 2005).

Gene disruption and replacement

The PRODIGE method for PCR product-mediated gene disruption was employed (Fig. 1A; Edlind *et al.*, 2005). Briefly, primers (80 mers; Table 3) were designed to precisely replace, after homologous recombination, a *C. glabrata* coding sequence (CDS) with the selection marker CDS. These primers consisted of *c.* 60 nucleotides at the 5′ end complementary to *C. glabrata* sequences directly upstream and downstream of the targeted CDS and *c.* 20 nucleotides at the 3′ end complementary to the *S. cerevisiae URA3* CDS contained in plasmid template pRS416. PCR products generated with these primers were used to transform *C. glabrata ura3* strains. Following selection on DOB-URA medium, transformants were screened by PCR with specific primer pairs (Table 3; Fig. 1A) to confirm replacement of the targeted CDS with *URA3* CDS. DNA was generally prepared by phenol extraction of glass bead-disrupted cells (Edlind *et al.*, 2005); some screens employed colony PCR in which a small volume of cells was added directly to the PCR mix.

For *PDR1* replacement, a PCR product representing the *PDR1* CDS plus 430–680 bp upstream and downstream sequence was amplified with primers PDR1uF-PDR1dR (Table 3) from 66032 or F15 genomic DNA. These products were used to transform 66032Δ*pdr1* strain with selection on 1 μg ml^{-1} cycloheximide-containing YPD plates. Colonies were screened as above with primer pair PDR1uF2-PDR1iR (Table 3; Fig. 4A).

Broth microdilution assay

Fresh overnight cultures from a single colony were diluted 1 : 100 in YPD, incubated for 3 h with aeration, and then counted in a haemocytometer and diluted again to 1×10^4 cells ml^{-1}. Aliquots of 100 μl were distributed to wells of a 96-well flat-bottomed plate, except for row A which received 200 μl. Inhibitor was added to row A to the desired concentration and then serially twofold diluted to rows B through G; row H served as inhibitor-free control. Plates were incubated at 35°C for the indicated times. Absorbance at 630 nm was read with a microplate reader; background due to medium was subtracted from all readings. The MIC (minimum inhibitory concentration) was defined as the lowest concentration inhibiting growth at least 80% relative to the drug-free control.

RNA hybridization

Log phase cultures in YPD at 35°C were adjusted to 3×10^6 cells ml^{-1} and incubated for an additional 3 h. In some studies, cultures were divided into equal portions to which

Table 3. Primers used in this study (grouped by application).

PRODIGE-based gene disruption	
PDR1-URA3F	5′-*GCCTTTTTTTTTAGAATATATTGGTAAAGTCATTCTTTAGC TACGTTATTGAGAGAAT*ATGTCGAAAGCTACATATAAGG-3′
PDR1-URA3R	5′-*TGATTTTTCAGATTAAATATA*AAAATTATACAGGCTATGCACA CTGTCTAAATTAATAGCATTAGTTTTGCTGGCCGCATC-3′
CDR1-URA3F	5′-*TACTTACAGGAAAAAGAATTTACAACTCTTGATATATACAA AGTAAAGAAAAGTAACA*ATGTCGAAAGCTACATATAAGG-3′
CDR1-URA3R	5′-*TTTTCCGAATGCAATATGTATTAATACCAGAGCCAGATTATG AGCGCAGGCTAAATAAA*TTAGTTTTGCTGGCCGCATC-3′
PCR screening and *PDR1* replacement	
PDR1uF	5′-GGCGTATTCATAGAATCCGAA-3′
PDR1uF2	5′-GGTCCTTCTAATAGTCATCTTT-3′
PDR1iR	5′-CCATAGTATTCGTCGAGAGCA-3′
PDR1dR	5′-GACCTCTGTGAAAAGCTACTG-3′
URA3iR	5′-CAGCAACAGGACTAGGATGAG-3′
CDR1uF	5′-GCAGCTATGAGTTGAGGAAG-3′
CDR1iR	5′-ACGCCACATCGGCATCCTT-3′
DNA Probes for RNA hybridization	
ACT1F	5′-TTGACAACGGTTCCGGTATG-3′
ACT1R	5′-CCGCATTCCGTAGTTCTAAG-3′
CDR1F	5′-ACAATGTCTCTTGCAAGTGAC-3′
CDR1R	5′-AAGTGTTTTCTGATGTGCTTT-3′
PDH1F	5′-GTGATGAACCCCGATGA-3′
PDH1R	5′-TTCTTGATCTCGTTGGGCGT-3′
PDR1F	5′-AGTGCCACCACTAAGTCACT-3′
PDR1R	5′-CCATAGTATTGCTGCAGAGCA
YLR346F	5′-GGAACTGAAACGCAGAACCA-3′
YLR346R	5′-ATCCTTCCATGTGTCGGCAT-3′
YOR1F	5′-GAACAAGCCACAGACGTATC-3′
YOR1R	5′-CAAATTGCCAAGATGGCTGG-3′
YNL134F	5′-CCACCATGAAAGCTGCTGTA-3′
YNL134R	5′-AACTTAGGATCAGCTGGCAG-3′
YML131F	5′-AATGAACCCACACCGGGTTA-3′
YML131R	5′-TTCACCAGTTGCATCAACCAT-3′
RTA1F	5′-CGTTCGCGGTGTTGTTTCTT-3′
RTA1R	5′-CATCTTCAATATCGGCTTCGA-3′
MEC3F	5′-TAGCGTCATTACGGAGCCTT-3′
MEC3R	5′-TATCGGGACCGCTTTCTTGT-3′
YJL163F	5′-TAGGTGCCTCGCATTCTGAT-3′
YJL163R	5′-ATCTTGCCAGCTAATCCAGG-3′
Real-time RT-PCR	
18SrtF	5′-TCGGCACCTTACGAGAAATCA-3′
18SrtR	5′-CGACCATACTCCCCCCAGA-3′
CDR1rtF	5′-CATACAAGAAACACCAAAGTCGGT-3′
CDR1rtR	5′-GAGACACGCTTACGTTCACCAC-3′
PDH1rtF	5′-ACGAGGAGGAAGACGACTACGA-3′
PDH1rtR	5′-CTTTACTGGAGAACTCATCGCTGTT-3′
CSR1rtF	5′-TGGATTTTTTCTCCCATCTGGA-3′
CSR1rtR	5′-ACCACAGGGTCAAGCCATTTT-3′
PDR1rtF	5′-TTTGACTCTGTTATGAGCGATTAC-3′
PDR1rtR	5′-TTCGGATTTTTCTGTGACAATGG-3′
KAD2rtF	5′-AACCCGCAGTCATCGTGG-3′
KAD2rtR	5′-CCTGTCTCTCAGTTCTTGGAAACC-3′
YOR1rtF	5′-CCATCGGTGCTTGTGTAATGTTA-3′
YOR1rtR	5′-TTGAGAGGCGTGGAAAAAATG-3′
RTA1rtF	5′-TCCTGTTTGTCATTAGGGTTAGGG-3′
RTA1rtR	5′-TGGCAATTTTGTTCTTATTCCTCAG-3′
QDR2rtF	5′-GACGAATGAGGACGAGGCTG-3′
QDR2rtR	5′-GGTTGGACCTGGTTCTGTAAATAGG-3′
SUT1rtF	5′-ACGAGAGCCAGAAGTTGATGG-3′
SUT1rtR	5′-TGGAGGCGATAGGAATTGGT-3′
RPN4rtF	5′-AGCCAGTATGCTGACCCGAG-3′
RPN4rtR	5′-ACACGCCACATCGCCC-3′
SAC7rtF	5′-CGCTGGAGACGCCTGG-3′
SAC7rtR	5′-TCGTATCCGCTTGCTGTTCC-3′
YBT1rtF	5′-AAGTGCTTCTTCCGCCTCATT-3′
YBT1rtR	5′-AACAGGAGCTGGTGTAGTACCCA-3′
MET8rtF	5′-TCCACCGCTATGCGATTTCT-3′
MET8rtR	5′-GGAGATGACCCATTGGATGAA-3′

either fluconazole or a comparable volume of DMSO was added, followed by incubation for the indicated times. In all studies, culture volumes corresponding to 3×10^7 cells were removed and centrifuged to pellet cells. RNA preparation and hybridization analysis were as previously described (Smith and Edlind, 2002). Briefly, cell pellets were suspended in sodium acetate-EDTA buffer and stored frozen. After thawing, RNA was extracted by vortexing in the presence of glass beads, SDS and buffer-saturated phenol alternating with incubation at 65°C for 10–15 min. Samples were cooled on ice and centrifuged, and RNA was ethanol precipitated from the aqueous phase. RNAs were dissolved in water and denatured in formaldehyde-SSPE with incubation for 15 min at 65°C. Either 40 μl (for *ACT1* probing) or 200 μl (for other probes) of denatured RNA (approximately 4 or 20 μg, respectively) was applied to nylon membrane by using a slot blot apparatus. Membranes were rinsed in SSPE, UV cross-linked, hybridized to purified PCR products (see Table 3 for primers) labelled with ^{32}P by random priming (Takara), and exposed to film.

Construction of C. glabrata *microarrays*

The nucleotide sequences corresponding to 5272 *C. glabrata* ORFs were downloaded from the Génolevures Consortium (http://cbi.labri.fr/Genolevures/about.php, Build 2). Following the Affymetrix Design Guide, two separate probe sets for each ORF were designed, each consisting of 13 perfect match and 13 mismatch overlapping 25 base oligonucleotides targeted to the 3′ 600 bp region. For ORFs $<$ 600 bp the sequence was divided in two equal segments for subsequent design procedures. For quality control and normalization purposes, we designed two to three additional probe sets spanning the *C. glabrata* 18 s rRNA, *TDH1* and *ACT1* genes in addition to standard Affymetrix controls (BioB, C, D, cre, DAP, PHE, LYS, THR). The probe selection was performed by the Chip Design group at Affymetrix, using their proprietary algorithm to calculate probe set scores, which includes a probe quality metric, cross-hybridization penalty, and gap penalty. The probe sets were then examined for cross-hybridization against all other sequences in the *C. glabrata* genome as well as a number of constitutively expressed genes and rRNA from other common organisms. Duplicate probesets are made to distinct regions of the ORF, thereby allowing two independent measurements of the mRNA level for that particular gene. *C. glabrata* custom Affymetrix NimbleExpress Arrays were manufactured by NimbleGen Systems (Albert *et al*., 2003) per our specification.

RNA preparation for microarrays

Total RNA was isolated using the hot SDS-phenol method (Schmitt *et al*., 1990). Frozen cells were suspended in 12 ml of 50 mM sodium acetate (pH 5.2), 10 mM EDTA at room temperature, after which 800 μl of 25% sodium dodecyl sulphate and 12 ml of acid phenol (Fisher Scientific) were added. This mixture was incubated 10 min at 65°C with vortexing each minute, cooled on ice for 5 min, and centrifuged for 15 min at 12 000 *g*. Supernatants were transferred to new tubes containing 15 ml of chloroform, mixed and centrifuged at $200 \times g$ for 10 min. The aqueous layer was removed to new tubes, RNA was precipitated with 1 vol isopropanol and 0.1 vol 2 M sodium acetate (pH 5.0), and then collected by centrifugation at 17 000 *g* for 35 min at 4°C. The RNA pellet was suspended in 10 ml of 70% ethanol, collected again by centrifugation, and suspended in diethyl pyrocarbonate-treated water.

cRNA synthesis and labelling

Immediately prior to cDNA synthesis, the purity and concentration of RNA samples were determined from A_{260}/A_{280} readings and RNA integrity was determined by capillary electrophoresis using the RNA 6000 Nano Laboratory-on-a-Chip kit and Bioanalyzer 2100 (Agilent Technologies) as per the manufacturer's instructions. First and second strand cDNA was synthesized from 15 μg total RNA using the SuperScript Double-Stranded cDNA Synthesis Kit (Invitrogen) and oligo-dT24-T7 primer (PrOligo) according to the manufacturer's instructions. cRNA was synthesized and labelled with biotinylated UTP and CTP by *in vitro* transcription using the T7 promoter-coupled double stranded cDNA as template and the Bioarray HighYield RNA Transcript Labelling Kit (ENZO Diagnostics). Double stranded cDNA synthesized from the previous steps was washed twice with 70% ethanol and suspended in 22 μl of Rnase-free water. The cDNA was incubated as recommended with reaction buffer, biotin-labelled ribonucleotides, dithtiothreitol, Rnase inhibitor mix and T7 RNA polymerase for 5 h at 37°C. The labelled cRNA was separated from unincorporated ribonucleotides by passing through a CHROMA SPIN-100 column (Clontech) and ethanol precipitated at –20°C overnight.

Oligonucleotide array hybridization and analysis

The cRNA pellet was suspended in 10 μl of Rnase-free water and 10 μg was fragmented by ion-mediated hydrolysis at 95°C for 35 min in 200 mM Tris-acetate (pH 8.1), 500 mM potassium acetate, 150 mM magnesium acetate. The fragmented cRNA was hybridized for 16 h at 45°C to the *C. glabrata* NimbleExpress GeneChip arrays. Arrays were washed at 25°C with $6 \times$ SSPE, 0.01% Tween 20 followed by a stringent wash at 50°C with 100 mM MES, 0.1 M NaCl, 0.01% Tween 20. Hybridizations and washes employed the Affymetrix Fluidics Station 450 using their standard EukGE-WS2v5 protocol. The arrays were then stained with phycoerythrein-conjugated streptavidin (Molecular Probes) and the fluorescence intensities were determined using the GCS 3000 high-resolution confocal laser scanner (Affymetrix). The scanned images were analysed using software resident in GeneChip Operating System v2.0 (GCOS; Affymetrix). Sample loading and variations in staining were standardized by scaling the average of the fluorescent intensities of all genes on an array to a constant target intensity (250). The signal intensity for each gene was calculated as the average intensity difference, represented by $[\Sigma(PM - MM)/(\text{number of probe pairs})]$, where PM and MM denote perfect-match and mismatch probes.

Microarray data analysis

The scaled gene expression values from GCOS software were imported into GeneSpring 7.2 software (Agilent Technologies) for preprocessing and data analysis. Probesets were deleted from subsequent analysis if they were called absent by the Affymetrix criterion and displayed an absolute value below 20 in all experiments. The expression value of each gene was normalized to the median expression of all genes in each chip as well as the median expression for that gene across all chips in the study. Pairwise comparison of gene expression was performed for each matched experiment (F15 vs. 66032). Genes were included in the final data set if their expression changed by at least twofold between strain F15 and strain 66032 in two independent experiments.

Quantitative real-time RT-PCR

First strand cDNAs were synthesized from 2 μg total RNA in a 21 μl reaction volume using the SuperScript First-Strand Synthesis System for RT-PCR (Invitrogen) as per the manufacturer's instructions. Quantitative real-time PCR was performed in triplicate using the 7000 Sequence Detection System (Applied Biosystems). Independent amplifications were performed using the same cDNA for both the gene of interest and 18S rRNA, using the SYBR Green PCR Master Mix (Applied Biosystems). Gene-specific primers were designed for the gene of interest and 18S rRNA using Primer Express software (Applied Biosystems) and the Oligo Analysis and Plotting Tool (Qiagen). The PCR conditions consisted of AmpliTaq Gold activation at 95°C for 10 min, followed by 40 cycles of denaturation at 95°C for 15 s and annealing/extension at 60°C for 1 min. A dissociation curve was generated at the end of each cycle to verify that a single product was amplified using software provided with the 7000 Sequence Detection System. The change in fluorescence of SYBR Green I dye in every cycle was monitored by the system software, and the threshold cycle (C_T) above background for each reaction was calculated. The C_T value of 18S rRNA was subtracted from that of the gene of interest to obtain a ΔC_T value. The ΔC_T value of an arbitrary calibrator (e.g. untreated sample) was subtracted from the ΔC_T value of each sample to obtain a $\Delta\Delta C_T$ value. The gene expression level relative to the calibrator was expressed as $2^{-\Delta\Delta CT}$.

Acknowledgements

We thank V. Pirrone for assistance with the heat shock assay, and J. Rex and B. Cormack for providing strains. Support was provided by NIH Grant AI047718 (to T.D.E.) and AI058145 (to P.D.R.).

References

Akins, R.A. (2005) An update on antifungal targets and mechanisms of resistance in *Candida albicans*. *Med Mycol* **43:** 285–318.

Albert, T.J., Norton, J., Ott, M., Richmond, T., Nuwaysir, K., Nuwaysir, E.F., *et al.* (2003) Light-directed 5′ → 3′ synthesis of complex oligonucleotide microarrays. *Nucleic Acids Res* **31:** e35.

Anderson, J.B., Sirjusingh, C., Parsons, A.B., Boone, C., Wickens, C., Cowen, L.E., and Kohn, L.M. (2003) Mode of selection and experimental evolution of antifungal drug resistance in *Saccharomyces cerevisiae*. *Genetics* **163:** 1287–1298.

Barns, S.M., Lane, D.J., Sogin, M.L., Bibeau, C., and Weisburg, B.G. (1991) Evolutionary relationships among pathogenic *Candida* species and relatives. *J Bacteriol* **173:** 2250–2255.

Bennett, J.E., Izumikawa, K., and Marr, K.A. (2004) Mechanism of increased fluconazole resistance in *Candida glabrata* during prophylaxis. *Antimicrob Agents Chemother* **48:** 1773–1777.

Brun, S., Dalle, F., Saulnier, P., Renier, G., Bonnin, A., Chabasse, D., and Bouchara, J.P. (2005) Biological consequences of petite mutations in *Candida glabrata*. *J Antimicrob Chemother* **56:** 307–314.

Carvajal, E., van den Hazel, H.B., Cybularz-Kolaczkowska, A., Balzi, A., and Goffeau, A. (1997) Molecular and phenotypic characterization of yeast *PDR1* mutants that show hyperactive transcription of various ABC multidrug transporter genes. *Mol Gen Genet* **256:** 406–415.

Cormack, B.P., and Falkow, S. (1999) Efficient homologous and illegitimate recombination in the opportunistic yeast pathogen *Candida glabrata*. *Genetics* **151:** 979–987.

Cui, Z., Hirata, D., Tsuchiya, E., Osada, H., and Miyakawa, T. (1996) The multidrup resistance-associated protein (MRP) subfamily (Yrs1/Yor1) of *Saccharomyces cerevisiae* is important for the tolerance to a broad range of organic anions. *J Biol Chem* **271:** 14712–14716.

DeRisi, J., van den Hazel, B., Marc, P., Balzi, E., Brown, P., Jacq, C., and Goffeau, A. (2000) Genome microarray analysis of transcriptional activation in multidrug resistance yeast mutants. *FEBS Lett* **470:** 156–160.

Devaux, F., Marc, P., Bouchoux, C., Delaveau, T., Hikkel, I., Potier, M.-C., and Jacq, C. (2001) An artificial transcription activator mimics the genome-wide properties of the yeast Pdrl transcription factor. *EMBO Rep* **2:** 493–498.

Diekema, D.J., Messer, S.A., Brueggemann, A.B., Coffman, S.L., Doern, G.V., Herwaldt, L.A., and Pfaller, M.A. (2002) Epidemiology of candidemia: 3-year results from the emerging infections and the epidemiology of Iowa organisms study. *J Clin Microbioil* **40:** 1298–1302.

Domergue, R., Castano, I., De Las Penas, A., Zupancic, M., Lockatell, V., Hebel, J.R., *et al.* (2005) Nicotinic acid limitation regulates silencing of *Candida* adhesins during UTI. *Science* **308:** 866–870.

Douglas, L.J. (2003) *Candida* biofilms and their role in infection. *Trends Microbiol* **11:** 30–36.

Dujon, B., Sherman, D., Fischer, G., Durrens, P., Casaregola, S., Lafontaine, I., *et al.* (2004) Genome evolution in yeasts. *Nature* **430:** 35–44.

Edlind, T.D., Henry, K.W., Vermitsky, J.-P., Edlind, M.P., Raj, S., and Katiyar, S.K. (2005) Promoter-dependent disruption of genes: simple, rapid, and specific PCR-based method with application to three different yeast. *Curr Gen* **48:** 117–125.

Gasch, A.P., Spellman, P.T., Kao, C.M., Carmel-Harel, O., Eisen, M.B., Storz, G., *et al.* (2000) Genomic expression programs in the response of yeast cells to environmental changes. *Mol Biol Cell* **11:** 4241–4257.

Goswami, D., Goswami, R., Banerjee, U., Dadhwal, V., Miglani, S., Lattif, A.A., and Kochupillai, N. (2006) Pattern of *Candida* species isolated from patients with diabetes mellitus and vulvovaginal candidiasis and their response to single dose oral fluconazole therapy. *J Infect* **52:** 111–117.

Grimoud, A.M., Lodter, J.P., Marty, N., Andrieu, S., Bocquet, H., Linas, M.D., *et al.* (2005) Improved oral hygiene and *Candida* species colonization level in geriatric patients. *Oral Dis* **11:** 163–169.

Izumikawa, K., Kakeya, J., Tsai, J.-F., Grimberg, B., and Bennett, J.E. (2003) Function of *Candida glabrata* ABC transporter gene, PDH1. *Yeast* **20:** 249–261.

Kaur, R., Domergue, R., Zupancic, M.L., and Cormack, B.P. (2005) A yeast by any other name: *Candida glabrata* and its interaction with the host. *Curr Opin Microbiol* **8:** 378–384.

Klingspor, L., Torngvist, E., Johansson, A., Petrini, B., Forsum, U., and Hedin, G. (2004) A prospective epidemiological survey of candidemia in Sweden. *Scand J Infect Dis* **36:** 52–55.

Kolaczkowska, A., and Goffeau, A. (1999) Regulation of pleiotropic drug resistance in yeast. *Drug Resist Updates* **2:** 403–414.

Kontoyiannis, D.P., Reddy, B.T., Hanna, H., Bodey, G.P., Tarrand, J., and Raad, I.I. (2002) Breakthrough candidemia in patients with cancer differs from *de novo* candidemia in host factors and *Candida* species but not intensity. *Infect Control Hosp Epidemiol* **23:** 542–545.

Mannhaupt, G., Schnall, R., Karpov, V., Vetter, I., and Feldmann, H. (1999) Rpn4p acts as a transcription factor binding to PACE, a nonamer box found upstream of 26S proteasomal and other genes in yeast. *FEBS Lett* **450:** 27–34.

Marchler-Bauer, A., and Bryant, S.H. (2004) CD-Search: protein domain annotations on the fly. *Nucleic Acids Res* **32:** W327–W331.

Miyazaki, H., Miyazaki, Y., Geber, A., Parkinson, T., Hitchcock, C., Falconer, D.J., *et al.* (1998) Fluconazole resistance associated with drug efflux and increased transcription of a drug transporter gene, *PDH1*, in *Candida glabrata*. *Antimicrob Agents Chemother* **42:** 1695–1701.

Nikawa, H., Egusa, H., Makihira, S., Nishimura, M., Ishida, K., Furukawa, M., and Hamada, T. (2003) A novel technique to evaluate the adhesion of *Candida* species to gingival epithelial cells. *Mycoses* **46:** 384–389.

Ostrosky-Zeichner, L., Rex, J.H., Pappa, P.G., Hamill, R.J., Larsen, R.A., Horowitz, H.W., *et al.* (2003) Antifungal susceptibility survey of 2,000 bloodstream *Candida* isolates in the United States. *Antimicrob Agents Chemother* **47:** 3149–3154.

Pfaller, M.A., Messer, S.A., Hollis, R.J., Jones, R.N., Doern, G.V., Brandt, M.E., and Hajjeh, R.A. (1999) Trends in species distribution and susceptibility to fluconazole among blood stream isolates of *Candida* species in the United States. *Diagn Microbiol Infect Dis* **33:** 217–222.

Pfaller, M.A., Messer, S.A., Boyken, L., Hollis, R.J., Rice, C., Tendolkar, S., and Diekema, D.J. (2004) *In vitro* activities of voriconazole, posaconazole, and fluconazole against 4,169 clinical isolates of *Candida spp. & Cryptococcus neoformans* collected during 2001 and 2002 in the ARTEMIS global antifungal surveillance program. *Diagn Microbiol Infect* **48:** 201–205.

Piper, P., Mahe, Y., Thompson, S., Pandjaitan, R., Holyack, C., Egner, R., *et al.* (1998) The Pdr12 ABC transporter is required for the development of weak organic acid resistance in yeast. *Embo J* **17:** 4257–4265.

Redding, S.W., Kirkpatrick, W.R., Saville, S., Coco, B.J., White, W., Fothergill, A., *et al.* (2003) Multiple patterns of resistance to fluconazole in *Candida glabrata* isolates from a patient with oropharyngeal candidiasis receiving head and neck radiation. *J Clin Microbiol* **41:** 619–622.

Rex, J.H., Nelson, P.W., Paetznick, V.L., Lozano-Chiu, M., Espinel-Ingroff, A., and Anaissie, E.J. (1998) Optimizing the correlation between results of testing *in vitro* and therapeutic outcome *in vivo* for fluconazole by testing critical isolates in a murine model of invasive candidiasis. *Antimicrob Agents Chemother* **42:** 129–134.

Richter, S.S., Galask, R.P., Messer, S.A., Hollis, R.J., Diekema, D.J., and Pfaller, M.A. (2005) Antifungal susceptibilities of *Candida* species causing vulvovaginitis and epidemiology of recurrent cases. *J Clin Microbiol* **30:** 2155–2162.

Safdar, A., and Armstrong, D. (2002) Prospective evaluation of *Candida* species colonization in hospitalized cancer patients: impact on short-term survival in recipients of marrow transplantation and patients with hematological malignancies. *Bone Marrow Transplant* **30:** 931–935.

Safdar, A., Chaturved, V., Cross, E.W., Park, S., Bernard, E.M., Armstrong, D., and Perlin, D.S. (2001) Prospective study of *Candida* species in patients at a comprehensive cancer center. *Antimicrob Agents Chemother* **45:** 2129–2133.

Safdar, A., Armstrong, D., Cross, E.W., and Perlin, D.S. (2002) Prospective epidemiologic analysis of triazole-resistant nosocomial *Candida glabrata* isolated from patients at a comprehensive cancer center. *Int J Infect Dis* **6:** 198–201.

Sanglard, D., Ischer, F., Calabrese, D., Majcherczyk, P.A., and Bille, J. (1999) The ATP binding cassette transporter gene CgCDR1 from *Candida glabrata* is involved in the resistance of clinical isolates to azole antifungal agents. *Antimicrob Agents Chemother* **43:** 2753–2765.

Sanglard, D., Ischer, F., and Bille, J. (2001) Role of ATP-binding-cassette transporter genes in high-frequency acquisition of resistance to azole antifungals in *Candida glabrate*. *Antimicrob Agents Chemother* **45:** 1174–1183.

Sanguinetti, M., Posteraro, B., Fiori, B., Ranno, S., Torelli, R., and Fadda, G. (2005) Mechanisms of azole resistance in clinical isolates of *Candida glabrata* collected during a hospital survey of antifungal resistance. *Antimicrob Agents Chemother* **49:** 668–679.

Schaller, M., Borelli, C., Korting, H.C., and Hube, B. (2005) Hydrolytic enzymes as virulence factors of *Candida albicans*. *Mycoses* **48:** 365–377.

Schmitt, M.E., Brown, T.A., and Trumpower, B.L. (1990) A rapid and simple method for preparation of RNA from *Saccharomyces cerevisiae*. *Nucleic Acids Res* **18:** 3091–3092.

Smith, W.L., and Edlind, T.D. (2002) Histone deacetylase inhibitors enhance *Candida albicans* sensitivity to azoles and related antifungals: correlation with reduction in *CDR* and *ERG* upregulation. *Antimicrob Agents Chemother* **46:** 3532–3539.

Tsai, H.-F., Krol, A.A., Sarti, K.E., and Bennett, J.E. (2006) *Candida glabrata PDR1*, a transcriptional regulator of a pleiotropic drug resistance network, mediates azole resistance in clinical isolates and petites mutants. *Antimicrob Agents Chemother* **50:** 1384–1392.

Vermitsky, J.-P., and Edlind, T.D. (2004) Azole resistance in *Candida glabrata*: coordinate upregulation of multidrug transporters and evidence for a Pdr1-like transcription factor. *Antimicrob Agents Chemother* **48:** 3773–3781.

Viscoli, C., Girmenia, C., Marinus, A., Collette, L., Martino, P., Vandercam, B., *et al.* (1999) Candidemia in cancer patients: a prospective, multicenter surveillance study by the Invasive Fungal infection Group (IFIG) of the European Organization for Research and Treatment of Cancer (EORTC). *Clin Infect Dis* **28:** 1071–1079.

